iNOS promotes CD24$^+$CD133$^+$ liver cancer stem cell phenotype through a TACE/ADAM17-dependent Notch signaling pathway

Ronghua Wang[a,b], Yawen Li[a], Allan Tsung[b], Hai Huang[b], Qiang Du[b], Muqing Yang[b], Meihong Deng[b], Si Xiong[a], Xiju Wang[a], Liyong Zhang[b], David A. Geller[b], Bin Cheng[a,1,2], and Timothy R. Billiar[b,1,2]

[a]Department of Gastroenterology and Hepatology, Tongji Hospital, Tongji Medical College, Huazhong University of Science and Technology, Wuhan 430030, China; and [b]Department of Surgery, University of Pittsburgh School of Medicine, Pittsburgh, PA 15213

The inducible nitric oxide synthase (iNOS) is associated with more aggressive solid tumors, including hepatocellular carcinoma (HCC). Notch signaling in cancer stem cells promotes cancer progression and requires Notch cleavage by ADAM (a disintegrin and metalloprotease) proteases. We hypothesized that iNOS/NO promotes Notch1 activation through TACE/ADAM17 activation in liver cancer stem cells (LCSCs), leading to a more aggressive cancer phenotype. Expression of the stem cell markers CD24 and CD133 in the tumors of patients with HCC was associated with greater iNOS expression and worse outcomes. The expression of iNOS in CD24$^+$CD133$^+$ LCSCs, but not CD24$^-$CD133$^-$ LCSCs, promoted Notch1 signaling and stemness characteristics in vitro and in vivo, as well as accelerating HCC initiation and tumor formation in the mouse xenograft tumor model. iNOS/NO led to Notch1 signaling through a pathway involving the soluble guanylyl cyclase/cGMP/PKG-dependent activation of TACE/ADAM17 and up-regulation of iRhom2 in LCSCs. In patients with HCC, higher TACE/ADAM17 expression and Notch1 activation correlated with poor prognosis. These findings link iNOS to Notch1 signaling in CD24$^+$CD133$^+$ LCSCs through the activation of TACE/ADAM17 and identify a mechanism for how iNOS contributes to progression of CD24$^+$CD133$^+$ HCC.

hepatocellular carcinoma | cancer stem cells | nitric oxide | Notch | TACE/ADAM17

Hepatocellular carcinoma (HCC) is closely associated with chronic inflammation, accumulation of genetic changes, alterations of the liver microenvironment, and generation of liver cancer stem cells (LCSCs) (1). Growing evidence supports the concept that tumor initiation can be driven by cancer stem cell (CSC) subsets that are responsible for tumor relapse, metastasis, and chemotherapy resistance (2). Therefore, identification of markers for LCSCs as well as signaling pathways activated in LCSCs could advance the development of liver cancer diagnosis and treatment strategies.

A series of studies suggests that continuous exposure to moderate to high concentrations of NO, produced by inducible NO synthase (iNOS), promotes neoplastic transformation (3–7) and tumor initiation (8–10). Downstream effects of NO production in tumors include DNA damage (3), enhanced angiogenesis and perfusion (4), chemotherapeutic resistance (11, 12), evasion of apoptosis (13, 14), enhanced cell proliferation (15), and increased inflammation and immune resistance (7, 10). Moreover, it has been shown that endothelial NO synthase (16) localizes near neoplastic cells displaying stem cell markers, and exogenous NO donors support stem cell signaling pathways in glioma cells (17). More recent findings have demonstrated that iNOS-generated NO is a distinctive feature of CSCs (18) that exhibit self-renewal capacity. These CSCs can differentiate into other tumor cell populations and seed the tumor in xenografts or at metastatic sites (19). These data suggest an integral role for NO and endogenous iNOS activity in the biology of CSCs.

The Notch signaling pathway promotes the self-renewal, differentiation, proliferation, survival, and migration of CSCs in

several malignancies (20, 21). Notch signaling promotes the progression of solid cancers (22) by driving angiogenesis (23) and maintaining a population of undifferentiated CSCs. Notch signaling is triggered when the Notch receptor is cleaved/activated at site 2 (S2; Val1711) (24) by ADAM (a disintegrin and metalloprotease) 10 or 17 proteases. Shedding of the Notch extracellular domain (NECD) by TACE/ADAM17 provides the signal for γ-secretases to cleave and release the Notch intracellular domain (NICD). NICD then interacts with the DNA-binding protein CSL and acts as a transcriptional activator for a set of genes that regulate cell proliferation, differentiation, epithelial-to-mesenchymal transition, and cell survival (25). However, it is unclear how TACE/ADAM17 is activated in tumors.

We recently reported that iNOS/NO activates TACE/ADAM17 in hepatocytes, leading to TNFR1 shedding (26). This was associated with iNOS/NO-mediated increases in iRhom2 levels, an intracellular protease that is localized to the endoplasmic reticulum and is critical for TACE/ADAM17 trafficking to the cell surface for Notch activation (27, 28). These studies raise the possibility that iNOS/NO plays an important role in CSC propagation through TACE/ADAM17 and Notch signaling.

MEDICAL SCIENCES

Here, we tested the hypothesis that iNOS regulates TACE/ADAM17-Notch1 signaling in LCSCs. We identified a population of CD24$^+$CD133$^+$ cells from HCC as iNOS$^+$ cells that possess stemness characteristics. We further demonstrated that iNOS activates Notch through TACE in CD24$^+$CD133$^+$ LCSCs through a cGMP/protein kinase G (PKG)-dependent mechanism. This NO-induced activation of Notch signaling accelerated HCC initiation and tumor formation in mice, while expression of CD24 and CD133, iNOS, or activated Notch in human HCC was correlated with worse clinical outcomes. Our data provide evidence of a mechanism for the tumorigenic effects of iNOS in promoting Notch1-mediated stemness in LCSCs.

Results

CD133$^+$CD24$^+$ HCC Cells Possess Stem/Progenitor Cell Characteristics.

CD133$^+$ cells possess higher colony-forming efficiency, pro-liferation rates, and capacity for tumorigenesis compared with CD133$^-$ cancer cells (29). CD24 is known to be up-regulated in residual chemotherapy-resistant tumors in mice, compared with bulk tumors, upon cisplatin treatment (30). Therefore, we hypothesized that CD133$^+$CD24$^+$ cells would contribute to the progression of HCC. We first investigated the relationship between the expression of CD133 and CD24 in tumors and clinical outcomes in 90 patients with HCC. Patients were separated into four groups based on CD24 and CD133 positivity: 12 (13%) cases of CD24$^+$CD133$^+$ expression, 28 (31%) cases of CD24$^+$CD133$^-$ expression, 10 (11%) cases of CD24$^-$CD133$^+$ expression, and 40 (45%) cases of CD24$^-$CD133$^-$ expression. Patients with CD24$^+$CD133$^+$ expression in their tumors had significantly shorter overall survival than those with CD24$^+$CD133$^-$, CD24$^-$CD133$^+$, or CD24$^-$CD133$^-$ expression ($P < 0.001$, log-rank test) (Fig. 1A).
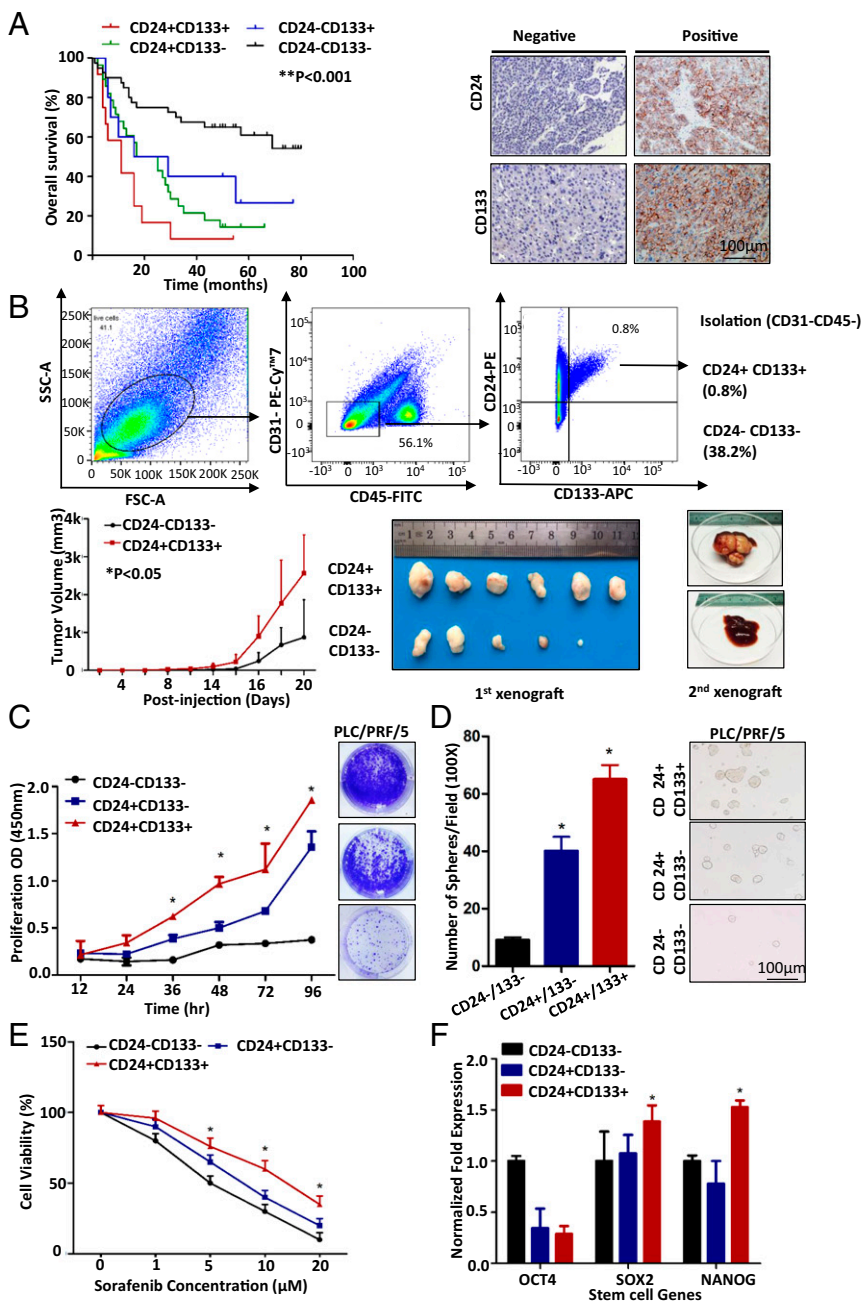
Fig. 1. CD24$^+$CD133$^+$ HCC cells possess stem/progenitor cell characteristics. (*A*) Overall survival in patients with HCC with CD24$^+$CD133$^+$ expression is significantly worse than that of CD24$^+$CD133$^-$, CD24$^-$CD133$^+$, and CD24$^-$CD133$^-$ expression groups (Kaplan–Meier analysis: log-rank test, **$P < 0.001$). (*B*) CD24$^+$CD133$^+$, CD24$^+$CD133$^-$, and CD24$^-$CD133$^-$ cells isolated by flow cytometry of human HCC specimens. (*Upper*) Pan-endothelial marker CD31 and the panleukocyte marker CD45 were used to eliminate potential contamination by endothelial or hematopoietic progenitor cells, respectively. CD24$^+$CD133$^+$ and CD24$^-$CD133$^-$ cells were isolated and inoculated s.c. into NOD/SCID mice. Greater s.c. tumor formation was observed using CD24$^+$CD133$^+$ than CD24$^-$CD133$^-$ cells ($n = 6$; *$P < 0.05$, t test). APC, allophycocyanin; FSC-A, forward scatter area; SSC-A, side scatter area. (*Lower*) CD24$^+$CD133$^+$ and CD24$^-$CD133$^-$ cells isolated from these tumors were then transplanted secondarily into the livers of new NOD/SCID recipients. Only CD133$^+$CD24$^+$ cells were capable of inducing liver tumor formation ($n = 12$; *$P < 0.05$, t test). (*C*) By colony formation assay on the sorted cells of PLC/PRF/5, CD24$^+$CD133$^+$ cells possessed a higher proliferation rate compared with CD24$^+$CD133$^-$ and CD24$^-$CD133$^-$ cells (*$P < 0.05$, t test). (*D*) By sphere formation assay, CD24$^+$CD133$^+$ cells possessed higher self-renewal ability in vitro compared with CD24$^+$CD133$^-$ and CD24$^-$CD133$^-$ cells (*$P < 0.05$, t test). (*E*) CD24$^+$CD133$^+$ cells exhibited chemotherapy resistance to sorafenib (0–20 µM for 48 h) compared with autologous CD24$^+$CD133$^-$ and CD24$^-$CD133$^-$ cells. (*$P < 0.05$, t test). (*F*) qPCR analysis shows that CD24$^+$CD133$^+$ cells had higher mRNA expression of stemness-associated genes, including Nanog and Sox2 (*$P < 0.05$, t test). Error bars represent SD from at least three independent experiments.

Stem-like characteristics were assessed in CD24$^+$CD133$^+$, CD24$^+$CD133$^-$, and CD24$^-$CD133$^-$ cells isolated by flow cytometry of human HCC specimens. To determine whether CD24$^+$CD133$^+$ HCC cells were more tumorigenic than CD24$^-$CD133$^-$ cells, purified cells were inoculated s.c. into nonobese diabetic (NOD)/SCID mice. A significantly higher tumor incidence was observed at 3 wk after CD24$^+$CD133$^+$ injection compared with injection with CD24$^-$CD133$^-$ cells (Fig. 1B, Lower). CD24$^+$CD133$^+$ and CD24$^-$CD133$^-$ cells isolated from these tumors were then transplanted secondarily into the livers of new NOD/SCID recipients. After 3 wk, all of the mice receiving secondary xenograft CD24$^+$CD133$^+$ cells, but not those injected with CD24$^-$CD133$^-$ cells, showed liver tumor formation that reconstituted the phenotypic heterogeneity of the primary xenografts, providing direct evidence of self-renewal of the CD24$^+$CD133$^+$ cells. Moreover, significantly more clones as well as larger hepatospheres were observed in cultures of CD24$^+$CD133$^+$ cells compared with cultures of CD24$^-$CD133$^-$ or CD24$^+$CD133$^-$ cells (Fig. 1 C and D). CD24$^+$CD133$^+$ cells showed significantly greater chemotherapy resistance to sorafenib compared with autologous CD24$^+$CD133$^-$ or CD24$^-$CD133$^-$ cells (Fig. 1E). Next, we found that CD24$^+$CD133$^+$ cell populations had higher expression of stemness-associated genes, including Nanog and Sox2 (Fig. 1F). Thus, CD24$^+$CD133$^+$ HCC not only showed worse outcomes in patients but cells from CD24$^+$CD133$^+$ tumors showed more aggressive tumor stem cell behavior.

iNOS-Directed CD24$^+$CD133$^+$ HCC Cell Tumor Initiation and Self-Renewal Capacity in Vitro and in Vivo. Tumor expression of iNOS is associated with more aggressive epithelial cancer (31). To determine the expression of iNOS mRNA and protein in LCSCs and non-LCSC subpopulations, we sorted CD24$^+$CD133$^+$ and CD24$^-$CD133$^-$ cell populations from freshly dissociated human HCC or HCC cell lines (HLE, MHCC-97H, PLC/PRF/5, and HepG2). The iNOS mRNA levels were higher in CD24$^+$CD133$^+$ LCSCs relative to non-LCSCs from primary human HCC as well as HCC cell lines (Fig. 2A and *SI Appendix*, Fig. S1A). Furthermore, iNOS protein levels [determined as mean fluorescence by immunohistochemistry (IHC)] were elevated in CD24$^+$CD133$^+$ ($n = 12$) cells compared with CD24$^-$CD133$^-$ ($n = 40$) cells derived from human tumors (Fig. 2A; $P < 0.05$, t test).
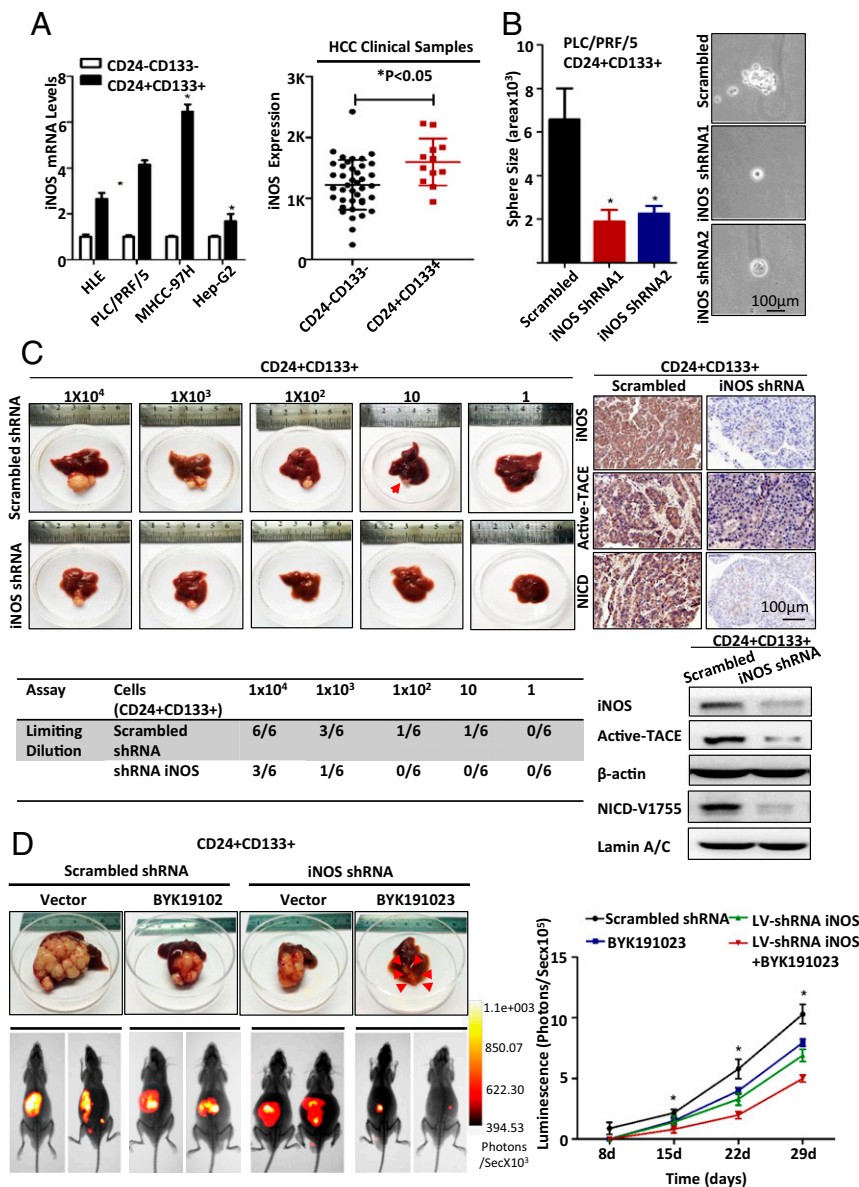
The higher expression of iNOS in CD24$^+$CD133$^+$ cells leads us to hypothesize that iNOS contributed to the stemness properties in CD24$^+$CD133$^+$ LCSCs. Lentiviral (Lv)-based shRNA-mediated knockdown of iNOS (*SI Appendix*, Fig. S1B) not only significantly decreased hepatosphere size in LCSCs derived from MHCC-97H cells but also dramatically attenuated the hepatosphere formation in the second- and third-generation cell cultures, compared with LCSCs treated with scrambled shRNA (Fig. 2B and *SI Appendix*, Fig. S1C). The effect of iNOS knockdown on LCSC tumorigenicity was also examined in a mouse orthotopic liver xenograft tumor model. To investigate the tumor-initiating capacity of CD24$^+$CD133$^+$ LCSCs, an orthotopic in vivo limiting dilution assay (employing 1×10^4, 1×10^3, 1×10^2, 10 cells, and 1 cell per mouse) was performed in NOD/SCID mice. Fig. 2C shows that as few as 10 CD24$^+$CD133$^+$ LCSCs transfected with scrambled shRNA could form tumors, whereas tumor formation required 1×10^3 CD24$^+$CD133$^+$ LCSCs transfected with iNOS shRNA. Moreover, the volume of tumors derived from iNOS shRNA cells was lower than that derived from scrambled shRNA cells. IHC and Western blots showed that tumors derived from iNOS shRNA cells exhibited less TACE and NICD than tumors derived from cells that received scrambled shRNA cells (Fig. 2C, Right). Consistent with these results, the iNOS inhibitors BYK191023 and 1400 W decreased TACE and Notch1 expression in CD24$^+$CD133$^+$ LCSCs (*SI Appendix*, Fig. S1D). Interestingly, the expression of CD24 and CD133, which was 95.1% and 92.5%, respectively, at

the time of injection, dropped to 20.1% and 2.1%, respectively, in the dispersed tumor cells subjected to flow cytometry at 4 wk. This change may reflect the differentiation of LCSCs to tumors cells and dilution of LCSCs as the tumors form. We found that shRNA iNOS actually decreased the frequency of LCSCs that express CD24 and CD133 over 72 h in vitro (*SI Appendix*, Fig. S1E). These results indicate that iNOS-targeted shRNA decreased the tumorigenicity of CD24$^+$CD133$^+$ LCSCs, and suggest that the iNOS/TACE/Notch1 signaling pathway may play an important role in the tumorigenic progress of LCSCs. Furthermore, iNOS sustains tumor stem cell markers in LCSCs.

We injected luciferase-expressing CD24$^+$CD133$^+$ LCSCs derived from iNOS shRNA or vector control (scrambled shRNA) clones into NOD/SCID mice ($n = 24$ per group) via the portal vein, and then monitored weekly for bioluminescent signals. To eliminate iNOS activity in the cancer microenvironment, half of iNOS shRNA and control group recipient mice ($n = 12$) received the iNOS inhibitor BYK191023 (31) (60 mg/kg) twice daily starting 1 wk after engraftment. Bioluminescent signals in livers from the BYK191023 group, iNOS shRNA group, or iNOS shRNA with BYK191023 group were weaker throughout the observation period than those from the control group (Fig. 2D; 29 d, $n = 12$). The incidence of tumor formation was 100% in the untreated control CD24$^+$CD133$^+$ group, but it was reduced to 66.7%, 50%, and 25% in the BYK191023, iNOS shRNA, and iNOS shRNA with BYK191023 groups, respectively (*SI Appendix*, Fig. S1F; 29 d, $n = 12$). Collectively, these data suggest that iNOS in both the LCSCs and the tumor microenvironment promote CD24$^+$CD133$^+$ HCC cell tumor initiation and raise the possibility that iNOS-directed therapeutics may represent an effective LCSC-targeted strategy for inhibiting tumor growth.

iNOS Promotes the CSC Phenotype and Tumorigenicity via Activating Notch1. A recent study demonstrated that NO enhances glioma stem cell self-renewal capacity (17). Therefore, we investigated whether NO could drive the self-renewal and tumorigenicity of CD24$^+$CD133$^+$ LCSCs by overexpressing iNOS/NO with an adenovirus vector (Ad)-iNOS or LV-iNOS vector (*SI Appendix*, Fig. S2A). Increased iNOS expression preferentially promoted hepatosphere formation and clone formation capacity in CD24$^+$CD133$^+$ LCSCs but had minimal effect on CD24$^-$CD133$^-$ HCC cells. The effects of iNOS overexpression in LCSCs were partly blocked by the iNOS inhibitor BYK191023 (10 μM) (Fig. 3 A and B). Interestingly, CSCs are protected from reactive oxygen species toxicity by expression of aldehyde dehydrogenase (ALDH) (32). We found that overexpression of iNOS increased the frequency of ALDH$^+$ HCC cells in culture from 11.8 to 38.3% at 72 h in CD24$^+$CD133$^+$ HCC cells (Fig. 3C). CD24$^+$CD133$^+$ MHCC-97H cells with stable iNOS overexpression [lentiviral vector (LV)-iNOS] or control transfected cells [LV-negative control (NC)] were injected s.c. into NOD/SCID mice. LV-iNOS MHCC-97H cells led to earlier tumor formation, as well as greater tumor growth at 2 wk, compared with control cells (MHCC-97H with LV-NC infection) (*SI Appendix*, Fig. S2B). Collectively, these data demonstrate that iNOS overexpression promotes the stemness potential of CSCs in vitro and in vivo.

Our previous study demonstrated that the Notch pathway is activated in LCSCs and inhibition of the Notch pathway in CSCs suppresses tumorigenicity, cell invasion, and migration (33, 34). We next analyzed the link between iNOS and Notch pathway activation in Ad-iNOS–transduced CD24$^+$CD133$^+$ LCSCs. CSL-luciferase reporter/promoter constructs, which can be activated by Notch signaling, were transiently transfected into CD24$^+$CD133$^+$ MHCC-97H cells. Overexpression of iNOS significantly increased luciferase activity in the CSL-luciferase–expressing cells relative to untreated control LCSCs derived from MHCC-97H and PLC/PRF/5 HCC cells (Fig. 3D; $P < 0.01$). Transduction with Ad-iNOS

Fig. 2. iNOS promoted CD133⁺CD24⁺ HCC cell tumor initiation and self-renewal capacity in vitro and in vivo. (*A*) qPCR and IHC analysis revealed higher iNOS expression in CD24⁺CD133⁺ cells (LCSCs) versus CD24⁻CD133⁻ cells (non-LCSCs) in HCC cell lines (HLE, PLC/PRF/5, MHCC-97H, and Hep-G2) and cells derived from primary human specimens (*n* = 40 and *n* = 12, respectively; **P* < 0.05, *t* test). (*B*) Lentiviral-based shRNA-mediated knockdown of iNOS (shRNA1 and shRNA2) significantly decreased hepatosphere size in LCSCs derived from MHCC-97H cells compared with the scrambled shRNA (*n* = 3; **P* < 0.05, *t* test). (*C*, *Left*) Orthotopic in vivo limiting dilution assay shows that the volumes and numbers of tumors derived from iNOS shRNA-treated cells were lower than the those of tumors derived from scrambled shRNA cells [red arrowhead points to a small HCC in the liver of an NOD/SCID mouse; tumors were assessed at 4 wk (*n* = 6)]. (*C*, *Right*) Moreover, IHC and Western blots showed that tumors derived from iNOS shRNA-targeted LCSCs exhibited less TACE and NICD than scrambled shRNA-treated cells. (*D*) Bioluminescent signals in livers from the BKY191023-treated (60 mg/kg twice daily) mice, iNOS shRNA group, or iNOS shRNA with BKY191023 group were much weaker than those from the scrambled shRNA control group (*n* = 12; **P* < 0.05, *t* test).

also led to an increase in mRNA levels for the Notch1 receptor and the Notch target gene Hes1 relative to controls (Fig. 3*E*). Overexpression of iNOS led to an increase in active NICD in the cell nucleus based on detection of the Notch1 cleavage product of γ-secretase at Val1755. The iNOS activity inhibitors BYK191023 (10 μM) and 1400 W (100 μM) blocked these effects of iNOS overexpression (Fig. 3*F*). These data indicate that the iNOS/NO pathway can activate the Notch pathway in LCSCs.

iNOS Required TACE/ADAM17 to Activate Notch Signaling in LCSCs. Having determined that iNOS activity leads to Notch1 receptor cleavage and activation, we next explored the mechanism of

iNOS-mediated Notch1 cleavage. TACE/ADAM17 (TNF-α converting enzyme) has previously been shown to cleave/activate Notch (35). We have shown previously that iNOS expression in hepatocytes leads to the activation and translocation of TACE to the plasma membrane (26), so we detected whether iNOS expression could activate TACE-dependent cleavage of Notch1. Here, we found that TACE activity was preferentially increased in CD24⁺CD133⁺ cells compared with CD24⁻CD133⁻ cells in response to iNOS overexpression (Fig. 4*A*). The inhibition of iNOS (1400 W; 100 μM) or TACE (TAPI-2, TNF protease inhibitor 2; 20 μM) prevented this increase in TACE activity. TACE mRNA levels were not changed by iNOS overexpression

Fig. 3. iNOS promotes the CSC phenotype and tumorigenicity via activating Notch1. Increased iNOS expression with the Ad-iNOS or LV-iNOS vector preferentially promoted CD24$^+$CD133$^+$ LCSC hepatosphere formation (*A*) and clone formation capacity (*B*) with minimal effects on CD24$^-$CD133$^-$ non-LCSCs. The effects of iNOS overexpression were partly blocked by the iNOS inhibitor BYK191023 (10 μM). (*C*) Overexpression of iNOS with Ad-iNOS promoted stemness phenotype by expanding the ALDEFLUOR (ALDH)-positive HCC cell population compared with CD24$^+$CD133$^+$ HCC cells infected with control Ad-LacZ (11.8–38.3%, 72 h). SSC-A, side scatter area. (*D*) Overexpression of iNOS activates Notch1 by inducing a significant increase in luciferase expression in the CSL-luciferase–expressing cells (38.3%) relative to untreated controls in CD24$^+$CD133$^+$ LCSCs (11.8%) derived from MHCC-97H HCC cells. (*E*) qPCR analysis showed that mRNA levels for Notch1 and Hes1 were significantly elevated relative to controls after transduction with Ad-iNOS (*P < 0.05, *t* test). (*F*) Quantification of Western blot analysis showed that iNOS increased the activation of the Notch1 signal pathway, and this increase was blocked by the iNOS inhibitors BYK191023 (10 μM) and 1400 W (100 μM) (*P < 0.05, *t* test).

(ratio of Ad-iNOS–transduced cells vs. controls: 1.180 ± 0.26). Notch activation measured as an increase in CSL-luciferase expression paralleled the increase in TACE activation induced by iNOS overexpression. The iNOS-induced increase in luciferase activity was blocked by inhibition of TACE activity or expression (TAPI-2 and TACE siRNA) (Fig. 4*B*). iNOS overexpression increased active TACE detected by Western blot, and this was

suppressed by TACE inhibition (TAPI-2) as well as pretreatment with TACE siRNA (Fig. 4*C*). While full-length Notch was not influenced by iNOS overexpression, the increases in nuclear cleaved Notch (measured as NICD Val1755) induced by Ad-iNOS transduction were prevented by inhibition of TACE with siRNA TACE or TAPI-2 (Fig. 4*C*). Using fluorescence IHC, we found that activated TACE (white) increased and colocalized

Fig. 4. iNOS is required in activation of TACE and Notch signaling in LCSCs. (*A*) TACE activation [expressed as activity in relative fluorescence units (RFU)] was significantly increased in CD24$^+$CD133$^+$ cells after Ad-iNOS transfection compared with Ad-iNOS–transduced CD24$^-$CD133$^-$ cells, and this elevation was prevented by inhibition of iNOS (1400 W; 100 µM), or TACE (TAPI-2; 20 µM) for 6 h. (*B*) CSL-luciferase expression, as a readout of Notch activation, was significantly increased after Ad-iNOS transduction (10 ng, 48 h, 20.1-fold). This increase was prevented by inhibition of TACE with TACE siRNA (100 ng, 24 h, 2.5-fold) and TAPI-2 (20 µM, 6 h, 5.5-fold). All luciferase values were normalized to Renilla activity (*$P < 0.05$, t test). RLU, relative luciferase activity. (*C*) Ad-iNOS significantly increased activated TACE and Hes1 expression in CD24$^+$CD133$^+$ PLC/PRF/5 cells, and the increases were attenuated by TAPI-2 (20 µM or 50 µM, 6 h) and TACE siRNA (20 ng or 50 ng, 24 h) in a dose-dependent manner. β-Actin and Lamin A/C antibody were used as loading controls. Numbers on Western blots correspond to relative quantification. (*D*) Activated TACE (white) was elevated and colocalized with iNOS (green) at the perinuclear and perimembrane regions in the cytoplasm in hepatospheres derived from Ad-iNOS–transduced CD24$^+$CD133$^+$ LCSCs. The increase in activated TACE was blocked by TAPI-2 (50 µM, 6 h).

with iNOS (green) in the perinuclear area and adjacent to the plasma membrane of Ad-iNOS–transduced CD24$^+$CD133$^+$ MHCC-97H cells (Fig. 4*D*). These results indicate that iNOS-dependent TACE activation leads to Notch1 receptor cleavage and Notch1 signaling.

TACE Binds to iRhom2 and Activates Notch Signaling in LCSCs in an iNOS/cGMP/PKG-Dependent Manner. NO signaling leads to the activation and translocation of TACE through the soluble guanylyl cyclase (sGC), cGMP, and PKG (17). To determine if the activation of TACE and Notch1 cleavage in LCSCs were dependent

on cGMP/PKG signaling, CD24$^+$CD133$^+$ LCSCs were transduced with Ad-iNOS or Ad-LacZ, and then exposed to the sGC inhibitor ODQ (10 µM) or PKG inhibitor KT5823 (20 µM). Inhibition of either sGC or PKG significantly attenuated the Ad-iNOS–induced increases in active TACE and NICD levels (Fig. 5*A*).

We then asked whether stimulation of cells with exogenous cGMP would increase activated TACE and Notch1 cleavage. A nonhydrolyzable cGMP analog and potent activator of PKG, 8-Br-PET-cGMP (Pet-cGMP; 800 µM), increased activated TACE and NICD levels in CD24$^+$CD133$^+$ LCSCs at 2 h, and this was blocked by the PKG inhibitor KT5823 (20 µM) (Fig. 5*B*). The

Wang et al.
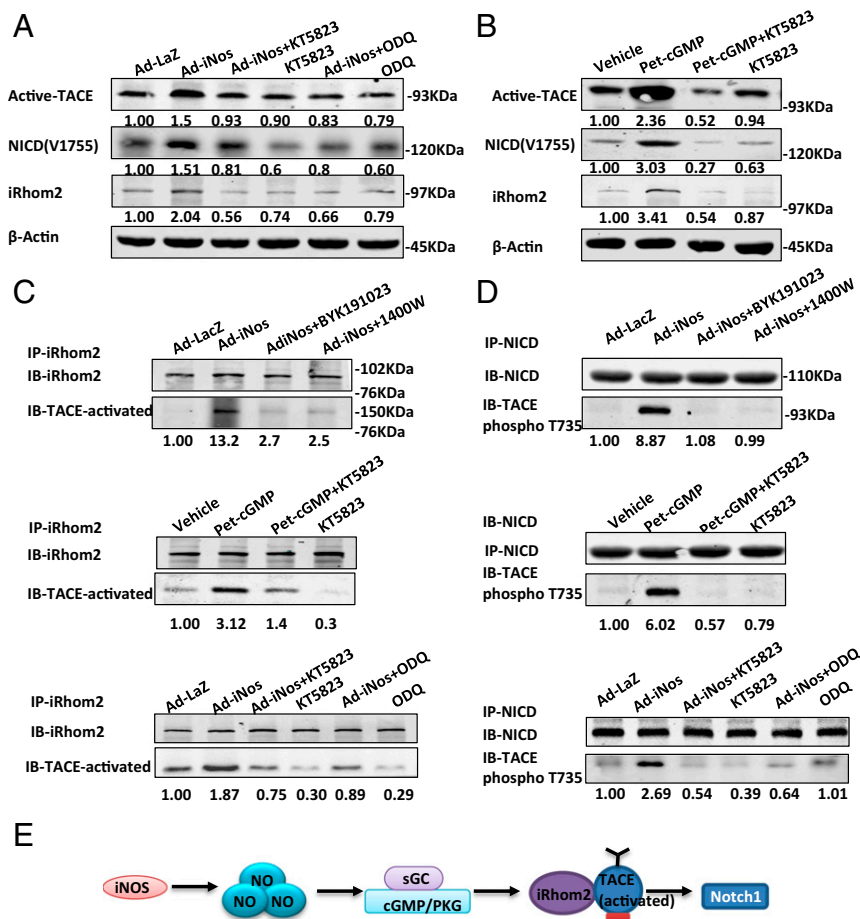
Fig. 5. TACE binds to iRhom2 and activates Notch signaling in LCSCs in an iNOS/cGMP-dependent manner. (*A*) Western blot analysis shows that over-expression of iNOS (Ad-iNOS) significantly increased levels of activated TACE, NICD-Val1755, and iRhom2 compared with Ad-LacZ controls. Moreover, in-hibition of either sGC (ODQ; 10 μM) or PKG (KT5823; 20 μM) significantly reduced activated TACE, NICD, and iRhom2 levels. (*B*) Western blot analysis shows that activation of PKG with Pet-cGMP (800 μM for 2 h) markedly increased levels of activated TACE, NICD, and iRhom2. Inhibition of PKG by KT5823 significantly prevented the elevation. (*C*) Immunoprecipitation (IP) experiments showed that the physical binding between activated-TACE and iRhom2 increased significantly after iNOS (Ad-iNOS) overexpression or PKG (PET-cGMP, 800 μM) activation, and the physical binding was partially attenuated by iNOS inhibition (BYK191023 10 μM or 1400 W 100 μM), sGC (ODQ, 10 μM), or PKG inhibition (KT5823, 20 μM). IB, immunoblotting. (*D*) IP experiments show that both iNOS overexpression and cGMP exposure lead to the binding of phosphorylated TACE (T735) with NICD. This physical interaction was blocked by iNOS inhibition (BYK191023; 10 μM or 1400 W; 100 μM), sGC (ODQ; 10 μM), or PKG inhibition (KT5823; 20 μM). (*E*) Summary of data. iNOS/NO drives TACE activation and Notch signaling through the sGC/cGMP/PKG pathway.

involvement of iRhom2 is essential to TACE maturation and trafficking from the endoplasmic reticulum to the cell surface in hematopoietic cells (27, 28). As shown in Fig. 5*A*, Ad-iNOS induced a marked increase in iRhom2 expression relative to the Ad-LacZ control group, and this increase was partially prevented by ODQ (10 μM) or KT5823 (20 μM). Pet-cGMP (800 μM) also increased iRhom2 expression, whereas the PKG inhibitor blocked the cGMP-induced up-regulation of iRhom2 in LCSCs (Fig. 5*B*).

Immunoprecipitation experiments revealed that the physical binding between TACE and iRhom2 increased significantly when iNOS was overexpressed (Fig. 5*C*). This interaction was partially attenuated by inhibition of iNOS (BYK191023 or 1400 W), sGC (ODQ), or PKG (KT5823), suggesting that the association of iRhom-2 and TACE is dependent on iNOS/cGMP/PKG (Fig. 5*C*). This was further confirmed by showing that KT5823 blocked Pet-cGMP–induced increases in iRhom2–TACE interaction. It is known that phosphorylation of TACE occurs at serine and threonine residues (36). As shown in Fig. 5*D*, iNOS overexpression or Pet-cGMP treatment led to serine/threonine phosphorylation of TACE (detected using an antiphosphothreonine

antibody) and an interaction between phosphorylated TACE and Notch1 in LCSCs. The effect of Pet-cGMP was blocked by PKG inhibition, and the impact of iNOS overexpression was prevented by inhibition of iNOS activity, sGC, and PKG. Collectively, these data indicate that iNOS/NO drives TACE activation and Notch signaling through the sGC/cGMP/PKG pathway (Fig. 5*E*). Moreover, this same signaling pathway increases the expression of iRhom2, which is essential to TACE maturation and trafficking (27, 28).

Elevated iNOS Expression Is Associated with Poor Prognosis in Patients with HCC and Positively Correlated with TACE and Notch1 Levels. The proliferative and tumorigenic effects of iNOS in LCSCs observed in vitro led us to evaluate whether iNOS, active TACE, or NICD expression in HCC correlated with tumor characteristics or survival in humans. A tumor histology array containing tissue from 90 human HCC specimens paired with normal liver from the same patients was used to perform IHC staining for CD24, CD133, iNOS, activated TACE/ADAM17, and NICD (Fig. 6*A*). Kaplan–Meier analysis showed that high iNOS and NICD expression was significantly associated with
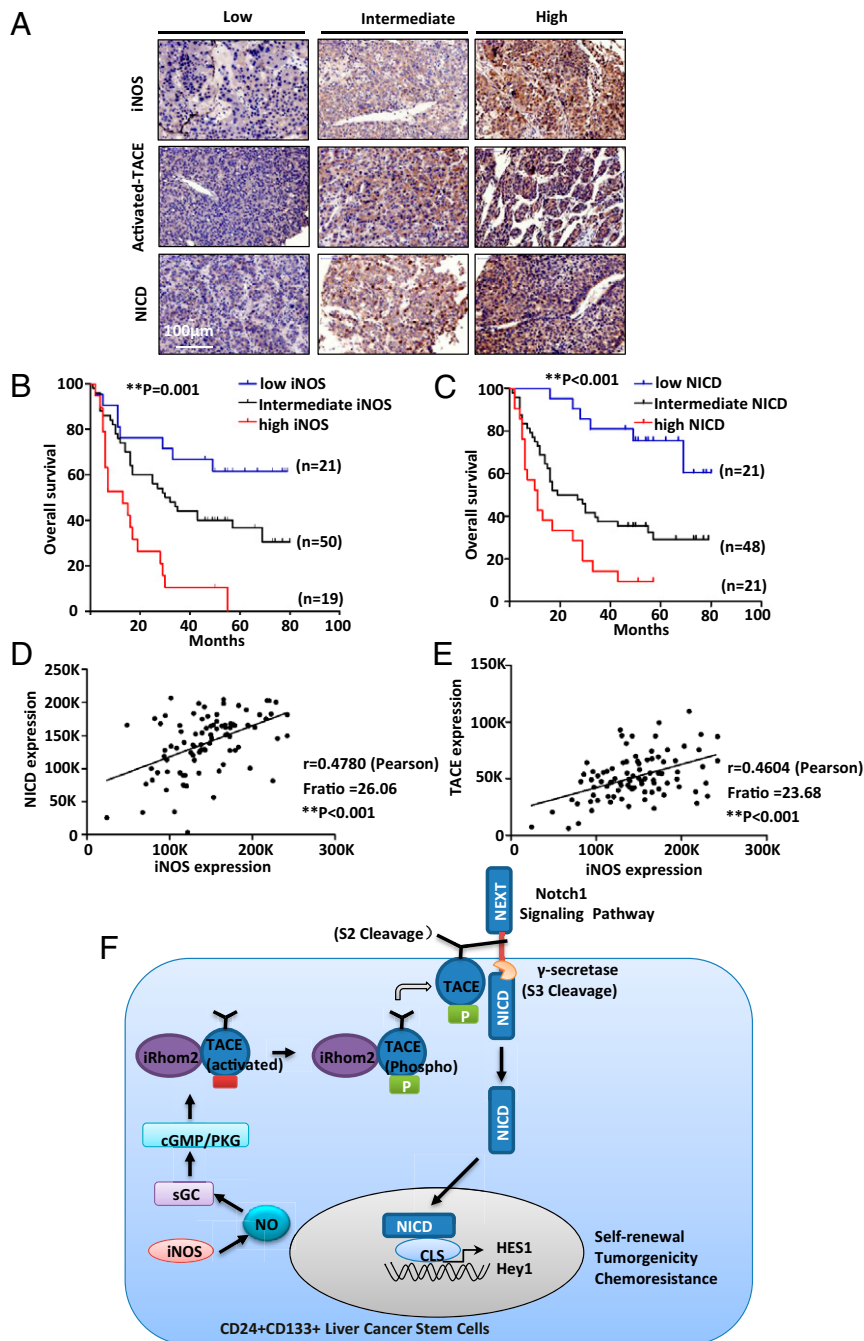
Fig. 6. Elevated iNOS expression is associated with poor prognosis in patients with HCC and is positively correlated with TACE and Notch1 levels. (*A*) Representative IHC images of high, intermediate, or low iNOS or NICD expression. The patients were designated as having high, intermediate, or low iNOS, Notch, or NICD expression. The Kaplan–Meier analysis showed that high iNOS (*B*) and NICD (*C*) expression was significantly associated with decreased survival of patients with HCC (log-rank test: **$P = 0.001$ and **$P < 0.001$, respectively). (*D* and *E*) iNOS in HCC is positively correlated with activated Notch1 (Pearson $r = 0.478$, **$P < 0.001$) and activated TACE (Pearson $r = 0.4604$, **$P < 0.001$). (*F*) Schematic diagram of our proposed model of iNOS/cGMP/PKG-induced TACE phosphorylation and activation of Notch1: iNOS is expressed in CD24$^+$CD133$^+$ LCSCs; iNOS enzyme generates NO, leading to the production of cGMP by sGC; and cGMP activates PKG, leading to the phosphorylation of TACE. Phosphorylated TACE undergoes a conformational change, which can serve as a binding partner for iRhom2; iRhom2 levels are increased by iNOS/NO/cGMP/PKG, and iRhom2 participates in the maturation of TACE; the interaction of iRhom2 with TACE facilitates the translocation of TACE to the cell surface to cleave membrane Notch1; and NICD then enters the nucleus, where it associates with the DNA-binding protein CSL to activate transcription of target genes such as Hes1.

lower survival of patients with HCC (Fig. 6 *B* and *C*; log-rank test: $P = 0.001$ and $P < 0.001$, respectively). Cox regression analysis showed that CD24 [hazard ratio (HR) = 2.355, $P = 0.009$], iNOS (HR = 2.028, $P = 0.0013$), active TACE (HR = 2.482, $P < 0.0001$), and NICD (HR = 2.487, $P = 0.0076$) are independent predictors of 7-y survival after adjustment for age at diagnosis, sex, TNM stage, and neoadjuvant therapy (*SI Appendix*, Table S1).

Next, we examined the relationship of iNOS and NICD with clinicopathological features, especially markers of tumor aggressiveness, in multivariate logistic regressions (Table 1). Both high iNOS and NICD expression correlated with elevated

Table 1. Association of high NOS2 expression with tumor characteristics

Clinicopathological characteristic	iNOS ($n = 90$)		NICD ($n = 90$)	
	OR (95%CI)	P	OR (95%CI)	P
Gender (male/female)	3.5 (0.86–14.22)	0.079	2.96 (0.74–11.83)	0.125
Age, y (<60/≥60)	1.63 (0.62–4.31)	0.324	1.40 (0.53–3.69)	0.494
Grade (1/2/3 stage)	1.61 (0.59–4.38)	0.350	1.89 (0.69–5.17)	0.213
Microsatellites (absence/presence)	2.38 (0.52–10.9)	0.261	**4.66 (1.08–21.93)**	**0.05***
Tumor size (<5 cm/≥5 cm)	1.38 (0.48–3.96)	0.550	0.54 (0.19–1.56)	0.256
Gross classification (massive/nodular/diffuse type)	0.78 (0.23–2.67)	0.686	0.66 (0.19–2.28)	0.513
Venous infiltration (absence/presence)	**4.80 (1.22–18.65)**	**0.025***	**14.24 (3.11–65.15)**	**0.0006****
TNM stage (low/high)	**3.72 (1.11–12.52)**	**0.034***	**3.37 (1.01–11.23)**	**0.048***
CD24 (low/high)	**2.80 (1.70–4.62)**	**0.032***	**2.53 (1.01–6.37)**	**0.049***
CD133 (low/high)	**1.36 (1.57–3.23)**	**0.049***	**2.55 (1.65–3.72)**	**0.033***

The IHC score of iNOS, TACE/Adam17, and activated Notch (NICD) in HCC was stratified into low, moderate, strong, and high for the analysis. "Low" is defined as expression less than onefold relative to mean values in normal tissue, whereas "high" is defined as expression greater than twofold relative to mean values in normal tissue. "Intermediate" expression is the range between low and high. Logistic regression was performed, with adjustments for age at diagnosis, gender, TNM stage, and neoadjuvant therapy. TNM stage was stratified into low (stage I/II) and high (stage III/IV). CD24 and CD133 counts were stratified into low (below the median) versus high (above the median).
*$P < 0.05$, **$P < 0.01$; significant difference (logistic regression, χ^2 test). Numbers in boldface font indicate statistical difference.

CD24 and CD133 expression. Whereas iNOS expression correlated significantly with venous infiltration [odds ratio (OR) = 4.80, $P = 0.025$] and advanced TNM stage (OR = 3.72, $P = 0.034$), high NICD expression correlated significantly with the presence of microsatellites (OR = 4.66, $P = 0.05$), venous infiltration (OR = 14.24, $P = 0.0006$), and advanced TNM stage (OR = 3.37, $P = 0.048$), after adjustment for age at diagnosis, sex, and neoadjuvant therapy.

To explore the correlation between iNOS, TACE, and Notch1, we evaluated the Pearson r coefficient between pairs of these variables. iNOS expression in HCC positively correlated with activated Notch1 (Fig. 6D; Pearson $r = 0.478$, $P < 0.001$) and with activated TACE (Fig. 6E; Pearson $r = 0.4604$, $P < 0.001$). These results further demonstrate that iNOS, activated TACE, and NICD may represent novel prognostic indices for predicting metastasis and overall survival in patients with HCC. Thus, our findings identified a correlation between iNOS, TACE, and Notch1 expression in outcomes of primary liver cancers. A schematic diagram of a proposed model of iNOS/cGMP/PKG-induced TACE phosphorylation and activation of Notch1 in CD24$^+$CD133$^+$ LCSCs is shown in Fig. 6F.

Discussion

In studies aimed at understanding the roles of LCSCs in HCC, we uncovered evidence that iNOS is expressed in an LCSC subset that expresses CD24 and CD133 and that these iNOS$^+$ cells are associated with a worse prognosis in humans with HCC. We provide evidence that iNOS may even support the expression of CD24 and CD133 in LCSCs. Our mechanistic studies indicate that iNOS/NO drives Notch signaling in CD24$^+$CD133$^+$ LCSCs and that iNOS and Notch signaling promote stem-like characteristics and more aggressive tumor growth in vivo. The activation of Notch1 is driven by NO/cGMP/PKG-mediated activation of TACE in association with the up-regulation of iRhom2. These studies provide a rationale for targeting the iNOS/NO/cGMP/PKG pathway in tumors with prominent iNOS$^+$ expression in CD24$^+$CD133$^+$ cells.

iNOS is associated with the progression of many solid tumors, such as human astrocytoma, human melanoma, and prostate cancer, as well as more advanced grades of human breast cancer (7, 9, 10). DNA damage induced by NO and its reaction products is also thought to contribute to tumor formation (37–39). An up-regulation of the tumor suppressor gene p53 was observed after the exposure of cells to NO donors (3, 4, 40), and mutated

p53 fails to suppress iNOS expression (41). Links have been made between iNOS and NO in promoting the stem cell compartment during neoplastic transformation in colon cancer and gliomas (17, 42). We go beyond these previous studies to show that CD24$^+$CD133$^+$ CSCs express iNOS in HCC. Furthermore, iNOS promoted stem-like characteristics and activation of Notch signaling through the NO/sGC/cGMP/PKG/TACE pathway in CD24$^+$CD133$^+$ LCSCs. iNOS activity in both the LCSCs and the microenvironment contributes to tumor progression in mice, suggesting that targeting iNOS in the entire tumor could have therapeutic benefit in HCC. While iNOS expression in stem cells may be part of an adaptation supporting stem cell renewal, iNOS expression in other cells is likely to be part of a proinflammatory tumor microenvironment (7).

Although the Notch1 pathway has been demonstrated in our previous study to play important roles in the maintenance and proliferation of LCSCs (33, 34, 43), we now provide evidence that iNOS/NO is linked to Notch1 activation in CSCs through the cGMP/PKG-dependent activation of TACE and up-regulation of iRhom2. This finding suggests that an important feature of LCSCs in more aggressive cancers is expression of all of the components of this signaling pathway.

ADAM proteases, such as ADAM17/TACE and ADAM10, cleave/activate Notch at S2 after ligands bind to the Notch receptor. Cell lineage-tracing experiments showed that ADAM10 controls intestinal crypt stem cell fate decisions by regulating Notch signaling (44). However, the requirement for ADAM17/TACE in Notch1 activation in LCSCs had not been defined. We determined that TACE controls LCSC survival and proliferation by activating Notch signaling. Moreover, TACE phosphorylation may be important in either the localization of TACE to the membrane or its activation (26, 27). Consistent with a role for phosphorylation in TACE translocation and/or activation, we show that the iNOS signaling pathway promotes TACE phosphorylation during Notch activation in LCSCs. Specifically, cGMP formation and PKG activation were important for activation of TACE, TACE phosphorylation, and TACE localization to the cell membrane, leading to NECD shedding. Previously, iRhom2 was found to facilitate the maturation and activation of TACE in hepatocytes (26). We extend these previous observations to show that iRhom2 is expressed and rapidly up-regulated in LCSCs through iNOS/NO/cGMP/PKG signaling. We implicate iRhom2 in Notch1 activation by showing the interaction between TACE and iRhom2 in response to the activity

of iNOS, sGC, cGMP, and PKG. The mechanistic links between iNOS/NO/cGMP/PKG signaling and ADAM17/TACE-mediated Notch activation in LCSC renewal were all made in vitro, which represents an important limitation of this work. It is also important to point out that the key experiments showing that iNOS and Notch promote liver cancer growth were performed in immune-deficient mice, and therefore must be interpreted with caution.

In summary, we demonstrate that Notch activation by iNOS/NO/sGC/cGMP/PKG-dependent TACE activation could be an important mechanism through which Notch promotes LCSC enrichment and function in HCC. Expression of iNOS and NICD was significantly associated with lower survival of patients with HCC. Our data also showed that iNOS is positively correlated with activated TACE and activated Notch1 in human HCC. The findings provided here could serve as an impetus for evaluation of iNOS/TACE/Notch1-directed therapies as a component of multimodal treatment regimens for human HCC.

Materials and Methods

Patient tissue histological array and isolation of primary human specimens were performed as follows: All tissue samples for the tissue histological array were obtained from consenting patients registered at the Tongji Hospital, Wuhan, China, between 2007 and 2009 and approved by the Ethics Committee (IRB ID TJ-C20150519). Clinical and pathological information (e.g., tumor receptor status) was obtained from medical records and pathology reports. Ninety pairs of HCC tissue samples, as well as their paired corresponding non-HCC tissues, were constructed as a liver cancer tissue microarray and used for IHC. Of the 90 patients in the database, 51 were known to be hepatitis B virus-positive and four were hepatitis C virus-positive. All clinical data are summarized in Table 1. All fresh human tissues used for isolation were acquired in accordance with the University of Pittsburgh IRB protocols (PRO08010372). All experiments involving human subjects were deidentified and approved by the University of Pittsburgh IRB and Tongji Hospital IRB. Tumor tissue was isolated and enzymatically dissociated with a collagenase Dissociation System (Worthington Biochemical). A detailed description of the materials and methods used in this study, including the assays and instrumentation used, animal model, and analysis methods, is provided in *SI Appendix*.

1. Magee JA, Piskounova E, Morrison SJ (2012) Cancer stem cells: Impact, heterogeneity, and uncertainty. *Cancer Cell* 21:283–296.
2. Ishizawa K, et al. (2010) Tumor-initiating cells are rare in many human tumors. *Cell Stem Cell* 7:279–282.
3. Lala PK, Chakraborty C (2001) Role of nitric oxide in carcinogenesis and tumour progression. *Lancet Oncol* 2:149–156.
4. Fukumura D, Kashiwagi S, Jain RK (2006) The role of nitric oxide in tumour progression. *Nat Rev Cancer* 6:521–534.
5. Ishimura N, Bronk SF, Gores GJ (2005) Inducible nitric oxide synthase up-regulates Notch-1 in mouse cholangiocytes: Implications for carcinogenesis. *Gastroenterology* 128:1354–1368.
6. Wink DA, et al. (1998) The role of nitric oxide chemistry in cancer treatment. *Biochemistry (Mosc)* 63:802–809.
7. Basudhar D, et al. (2017) Coexpression of NOS2 and COX2 accelerates tumor growth and reduces survival in estrogen receptor-negative breast cancer. *Proc Natl Acad Sci USA* 114:13030–13035.
8. Williams EL, Djamgoz MB (2005) Nitric oxide and metastatic cell behaviour. *BioEssays* 27:1228–1238.
9. Granados-Principal S, et al. (2015) Inhibition of iNOS as a novel effective targeted therapy against triple-negative breast cancer. *Breast Cancer Res* 17:25.
10. Davila-Gonzalez D, Chang JC, Billiar TR (2017) NO and COX2: Dual targeting for aggressive cancers. *Proc Natl Acad Sci USA* 114:13591–13593.
11. Fetz V, et al. (2009) Inducible NO synthase confers chemoresistance in head and neck cancer by modulating survivin. *Int J Cancer* 124:2033–2041.
12. Yang DI, Yin JH, Mishra S, Mishra R, Hsu CY (2002) NO-mediated chemoresistance in C6 glioma cells. *Ann N Y Acad Sci* 962:8–17.
13. Engels K, et al. (2008) NO signaling confers cytoprotectivity through the survivin network in ovarian carcinomas. *Cancer Res* 68:5159–5166.
14. Levesque MC, et al. (2003) IL-4 and interferon gamma regulate expression of inducible nitric oxide synthase in chronic lymphocytic leukemia cells. *Leukemia* 17:442–460.
15. Lim KJ, Bisht S, Bar EE, Maitra A, Eberhart CG (2011) A polymeric nanoparticle formulation of curcumin inhibits growth, clonogenicity and stem-like fraction in malignant brain tumors. *Cancer Biol Ther* 11:464–473.
16. Kashiwagi S, et al. (2008) Perivascular nitric oxide gradients normalize tumor vasculature. *Nat Med* 14:255–257.
17. Charles N, et al. (2010) Perivascular nitric oxide activates notch signaling and promotes stem-like character in PDGF-induced glioma cells. *Cell Stem Cell* 6:141–152.
18. Eyler CE, et al. (2011) Glioma stem cell proliferation and tumor growth are promoted by nitric oxide synthase-2. *Cell* 146:53–66.
19. Reya T, Morrison SJ, Clarke MF, Weissman IL (2001) Stem cells, cancer, and cancer stem cells. *Nature* 414:105–111.
20. Androutsellis-Theotokis A, et al. (2006) Notch signalling regulates stem cell numbers in vitro and in vivo. *Nature* 442:823–826.
21. Fan X, et al. (2010) NOTCH pathway blockade depletes CD133-positive glioblastoma cells and inhibits growth of tumor neurospheres and xenografts. *Stem Cells* 28:5–16.
22. Ranganathan P, Weaver KL, Capobianco AJ (2011) Notch signalling in solid tumours: A little bit of everything but not all the time. *Nat Rev Cancer* 11:338–351.
23. Roca C, Adams RH (2007) Regulation of vascular morphogenesis by Notch signaling. *Genes Dev* 21:2511–2524.
24. Bray SJ (2006) Notch signalling: A simple pathway becomes complex. *Nat Rev Mol Cell Biol* 7:678–689.
25. Kopan R, Ilagan MX (2009) The canonical Notch signaling pathway: Unfolding the activation mechanism. *Cell* 137:216–233.
26. Chanthaphavong RS, Loughran PA, Lee TY, Scott MJ, Billiar TR (2012) A role for cGMP in inducible nitric-oxide synthase (iNOS)-induced tumor necrosis factor (TNF) α-converting enzyme (TACE/ADAM17) activation, translocation, and TNF receptor 1 (TNFR1) shedding in hepatocytes. *J Biol Chem* 287:35887–35898.
27. McIlwain DR, et al. (2012) iRhom2 regulation of TACE controls TNF-mediated protection against Listeria and responses to LPS. *Science* 335:229–232.
28. Adrain C, Zettl M, Christova Y, Taylor N, Freeman M (2012) Tumor necrosis factor signaling requires iRhom2 to promote trafficking and activation of TACE. *Science* 335:225–228.
29. Ma S, et al. (2010) miR-130b promotes CD133(+) liver tumor-initiating cell growth and self-renewal via tumor protein 53-induced nuclear protein 1. *Cell Stem Cell* 7:694–707.
30. Lee TK, et al. (2011) CD24(+) liver tumor-initiating cells drive self-renewal and tumor initiation through STAT3-mediated NANOG regulation. *Cell Stem Cell* 9:50–63.
31. Du Q, et al. (2013) Nitric oxide production upregulates Wnt/β-catenin signaling by inhibiting Dickkopf-1. *Cancer Res* 73:6526–6537.
32. Raha D, et al. (2014) The cancer stem cell marker aldehyde dehydrogenase is required to maintain a drug-tolerant tumor cell subpopulation. *Cancer Res* 74:3579–3590.
33. Luo J, et al. (2016) The Notch pathway promotes the cancer stem cell characteristics of CD90+ cells in hepatocellular carcinoma. *Oncotarget* 7:9525–9537.
34. Wang R, et al. (2016) Notch and Wnt/β-catenin signaling pathway play important roles in activating liver cancer stem cells. *Oncotarget* 7:5754–5768.
35. Brou C, et al. (2000) A novel proteolytic cleavage involved in Notch signaling: The role of the disintegrin-metalloprotease TACE. *Mol Cell* 5:207–216.
36. Díaz-Rodríguez E, Montero JC, Esparís-Ogando A, Yuste L, Pandiella A (2002) Extracellular signal-regulated kinase phosphorylates tumor necrosis factor alpha-converting enzyme at threonine 735: A potential role in regulated shedding. *Mol Biol Cell* 13:2031–2044.
37. Sohn JJ, et al. (2012) Macrophages, nitric oxide and microRNAs are associated with DNA damage response pathway and senescence in inflammatory bowel disease. *PLoS One* 7:e44156.
38. Okayama H, et al. (2013) NOS2 enhances KRAS-induced lung carcinogenesis, inflammation and microRNA-21 expression. *Int J Cancer* 132:9–18.
39. Wink DA, et al. (2015) The oncogenic properties of the redox inflammatory protein inducible nitric oxide synthase in ER(-) breast cancer. *Redox Biol* 5:413.
40. Burney S, Niles JC, Dedon PC, Tannenbaum SR (1999) DNA damage in deoxynucleosides and oligonucleotides treated with peroxynitrite. *Chem Res Toxicol* 12:513–520.
41. Hussain SP, et al. (2000) Increased p53 mutation load in nontumorous human liver of wilson disease and hemochromatosis: Oxyradical overload diseases. *Proc Natl Acad Sci USA* 97:12770–12775.
42. Chan KS, et al. (2009) Identification, molecular characterization, clinical prognosis, and therapeutic targeting of human bladder tumor-initiating cells. *Proc Natl Acad Sci USA* 106:14016–14021.
43. Sun Q, et al. (2014) Notch1 promotes hepatitis B virus X protein-induced hepatocarcinogenesis via Wnt/β-catenin pathway. *Int J Oncol* 45:1638–1648.
44. Tsai YH, et al. (2014) ADAM10 regulates Notch function in intestinal stem cells of mice. *Gastroenterology* 147:822–834 e813.